Comparison of Multisine Measurements from Instrumentation Capable of Nonlinear System Characterization[∗]

Kate A. Remley[1], Paul D. Hale[2], David I. Bergman[3], Darryl Keenan[2]
National Institute of Standards and Technology
[1]Electromagnetics Division, [2]Optoelectronics Division, [3]Quantum Electrical Metrology Division
remley, hale@boulder.nist.gov, bergman@eeel.nist.gov

Abstract—We compare measurements of simple multisines using instruments capable of characterizing both magnitude and relative phase of the measured signals. The three instruments we compared reported relative phase measurements within a few degrees of each other with a standard deviation of less than a degree at microwave frequencies for both wide and narrow modulation bandwidths.

Key Words—digital sampling oscilloscope, vector signal analyzer, sampling waveform analyzer, time-base correction, phase detrending, multisine, wireless systems

I. INTRODUCTION

We describe measurements of multisine signals performed with three different instruments. Each instrument is capable of measuring both the magnitude and relative phase of the frequency components of bandpass multisine signals. While many instruments—including spectrum analyzers, vector network analyzers, and power meters—are capable of measuring the magnitudes of the frequency components and distortion products of multisines, at present only a few instruments can measure the relative phase. Accurate measurement of both magnitude and phase distortion is critical for characterizing distortion from circuits and systems that contain nonlinear elements. Our results provide an indication of how well these measurements can be carried out using today's instrumentation.

We chose to measure multisine signals because they can be designed to approximate digital signals used in wireless systems [1]. In addition, they are periodic and consist of discrete tones, enabling straightforward measurement and data analysis. For these reasons, multisines can easily be used as bandpass test and calibration signals to help to predict system performance.

We measured multisines generated by a vector signal generator (VSG) with three instruments: a timebase-error-corrected Digital Sampling Oscilloscope [2,3] with 50 GHz bandwidth, the NIST Sampling Waveform Analyzer [4,5] with 5.5 GHz measurement bandwidth, and a vector signal analyzer with 36 MHz bandwidth. All three instruments reported relative phase measurements within a degree or two of each other at microwave frequencies for both wideband (defined here as greater than 20 MHz) and narrowband (less than 20 MHz) modulation bandwidths. Comparing measurements gives us confidence in our relative phase measurements. As will be shown, these relative phase measurements can then be used to characterize equipment and carry out improved experiment design.

II. THE MULTISINES

We compare measurements of simple multisines having 3 to 33 frequency components and simple phase relationships. Their characteristics are shown in Table I. Repeat measurements of these test signals clearly illustrate several characteristics of interest for the instruments we

---

[∗] Publication of the U.S. Government, not subject to copyright in the United States.

Table I: Characteristics of the multisines we measured in this comparison, where Δf is the frequency spacing between tones, Δt is the nominal time between samples when measured by the DSO and SWA measurements. The number of envelope cycles is given by $t_{\text{final}}/\Delta f$. The carrier frequency for all measurements was 1 GHz, and the total average power in each multisine was -20 dBm.

Number of Tones	Δf	Relative Phase	Δt	t_{final}	Envelope Cycles
3	40 MHz	constant	50 ps	250 ns	10
5	20 MHz	constant	50 ps	250 ns	5
5	20 MHz	Schroeder	50 ps	250 ns	5
3	2.5 MHz	constant	100 ps	2 µs	5
4	2.5 MHz	constant	100 ps	2 µs	5
9	2.5 MHz	Schroeder	100 ps	2 µs	5
13	2.5 MHz	Schroeder	100 ps	2 µs	5
33	2.5 MHz	Schroeder	100 ps	2 µs	5

compared: statistical variations in magnitude and phase between measurements, harmonic distortion, and signal-to-noise levels.

The multisines were generated on a vector signal generator (VSG) using the front-panel controls. For each multisine, we collected 100 sets of measurements. To minimize harmonic distortion from the vector signal generator we set the total power in each multisine to -20 dBm.

In Table I, "constant" relative phase refers to a zero-degree phase difference between all tones (phase of each tone equals zero at time $t = t_{\text{ref}}$), "Schroeder" relative phases refer to N tones whose relative phases (in radians) are defined by [6]

$$\phi_k = \frac{k(k-1)\pi}{N}, \quad k = 1, 2, \ldots, N .$$

(1)

To compare the measured phase components from each instrument to those specified on the VSG, we applied a detrending algorithm [7] to remove the arbitrary time delay introduced by the instrumentation and cabling. The detrending algorithm was applied to the phase component of the complex Fourier coefficients of the transformed multisine. The algorithm finds the time in the measured multisine envelope where the mean-squared error between the specified phases and the measured phases is minimized. It first finds a rough time estimate based on an analytic expression, and then carries out an iterative search to minimize the mean-square error. The minimization procedure is necessary since the measured phases are generally somewhat different from the specified ones, and an analytic expression typically cannot account for the random and systematic effects that cause these differences [7].

We next describe some particular issues associated with the measurement of multisines using the three instruments. We then compare measurement results and demonstrate the usefulness of our ability to accurately characterize the vector signal generator.

III. Broadband Multisine Measurements

A. The Sampling Oscilloscope and the Sampling Waveform Analyzer

We first look at measurements made with two full-spectrum (as opposed to bandpass), time-domain instruments: the NIST Sampling Waveform Analyzer (SWA) and the Digital Sampling Oscilloscope (DSO). Although both of these instruments sample and digitize the signal being measured, their internal architectures differ significantly. The DSO utilizes a very fast sample-and-hold architecture, while the SWA is based upon a sampling comparator design. Both instruments have existing uncertainty analyses that may eventually be extended to multisine measurements, making them candidates for use in calibration of vector signal generators and other types of receivers, such as the vector signal analyzer (VSA). Both can measure multisines having modulation bandwidths greater than the 80 MHz limit of our signal generator. This capability is useful in the characterization of broadband wireless systems.

For the first three multisines shown in Table I, we triggered the DSO using the 10 MHz reference signal output from the vector signal generator. The SWA was triggered using the coherent carrier output frequency divided down to approximately 100 kHz. For the multisines with narrower frequency spacing, we used a frequency divider to trigger each instrument on the multisine envelope cycle. The trigger signals were sharpened to minimize jitter.

The data were acquired in the time domain then transformed to the frequency domain. We carried out this transformation by applying a Fourier Transform, which we define as $F(\omega) = \int_{-\infty}^{\infty} f(t)e^{-j\omega t}dt$, with $\omega = 2\pi f$ and f the frequency in Hertz. In our numerical computations we used a time- and frequency-discretized version of the Fourier transform, referred to as the Discrete Fourier Transform (DFT). To minimize spectral leakage, our time record always consisted of an integer number of envelope periods, shown in the last column of Table I. For example, if Δf was 20 MHz, then the envelope period corresponded to $1/\Delta f = 50$ ns and our time record was five times that, or 250 ns. Time-domain waveforms and spectra measured with these instruments for the 5-tone, 20 MHz-spaced multisine (row two of Table I) are shown in Fig. 1.

(a)   (b)
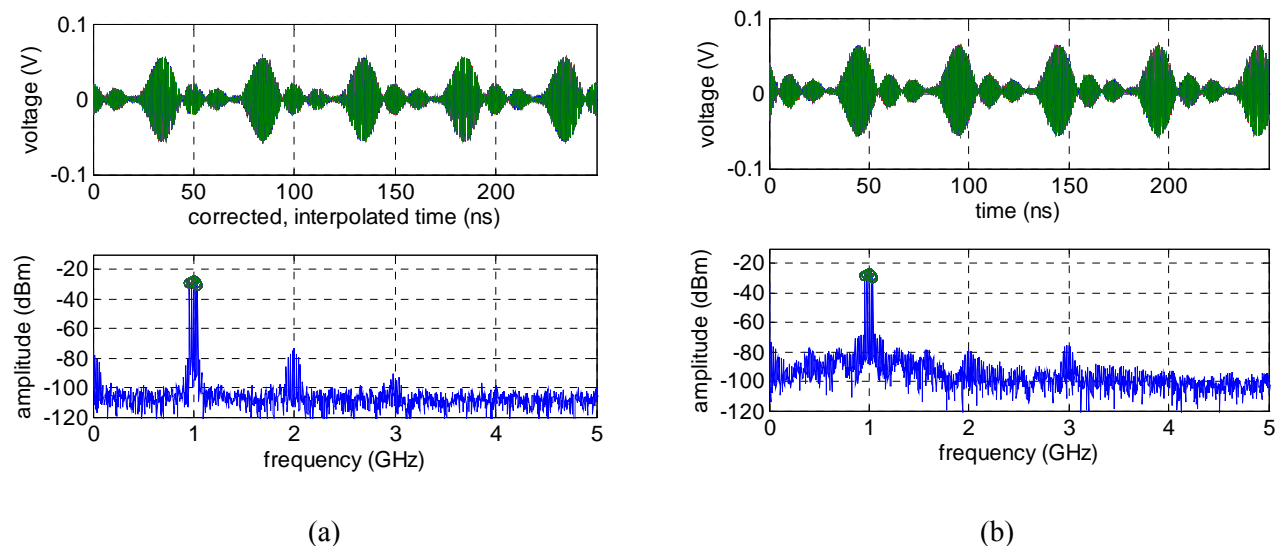
Figure 1: Time- (upper) and frequency-domain (lower) plots of a 5-tone multisine with $\Delta f = 20$ MHz, specified relative phases: 0°, 0°, 0°, 0°, 0°, (a) DSO measurement; (b) SWA measurement. Lower plots show the DFT of the average of 100 waveform measurements and circles show the multisine's frequency components.

The lower plots in Fig. 1 show the DFT of the average of 100 measurements from each of the instruments. Time-domain averaging can greatly improve the dynamic range in these instruments as compared to traditional frequency-domain averaging employed by spectrum analyzers. The upper graphs of Fig. 2 plot the signal-to-noise-and-distortion (SINAD) vs. number of measurements (runs) for the spectra shown in the lower plots, illustrating the improvement in apparent noise floor achieved with time-domain averaging. Frequency-domain averaging is illustrated in the lower plots of Fig. 2 by the thin (red) curve. SINAD is defined as the ratio of the signal-plus-noise-plus-distortion to the noise-plus-distortion. SINAD may be calculated in either the time or frequency domains. We performed our calculations in the frequency domain by finding the total average power in the measured spectrum, finding the noise-plus-distortion power by subtracting off the power in the multisine, and taking the ratio. Expressed in watts

$$\text{SINAD} = P_{\text{total}} \Big/ P_{\text{noise+dist}} , \tag{2}$$

where

$$P_{\text{noise+dist}} = P_{\text{total}} - P_{\text{multisine}} . \tag{3}$$

B. The Oscilloscope Measurements

For the oscilloscope measurements, time-base error correction [2,3] was carried out by making simultaneous measurements of the multisine as well as unmodulated in-phase and quadrature carrier-frequency signals on additional oscilloscope channels. This was done by sampling the coherent carrier output on the rear panel of our VSG both directly and with a phase shift of approximately 90° through a hybrid coupler. The time-base and jitter correction algorithm provides a corrected time record with a non-equally spaced increment. We used linear

(a)   (b)
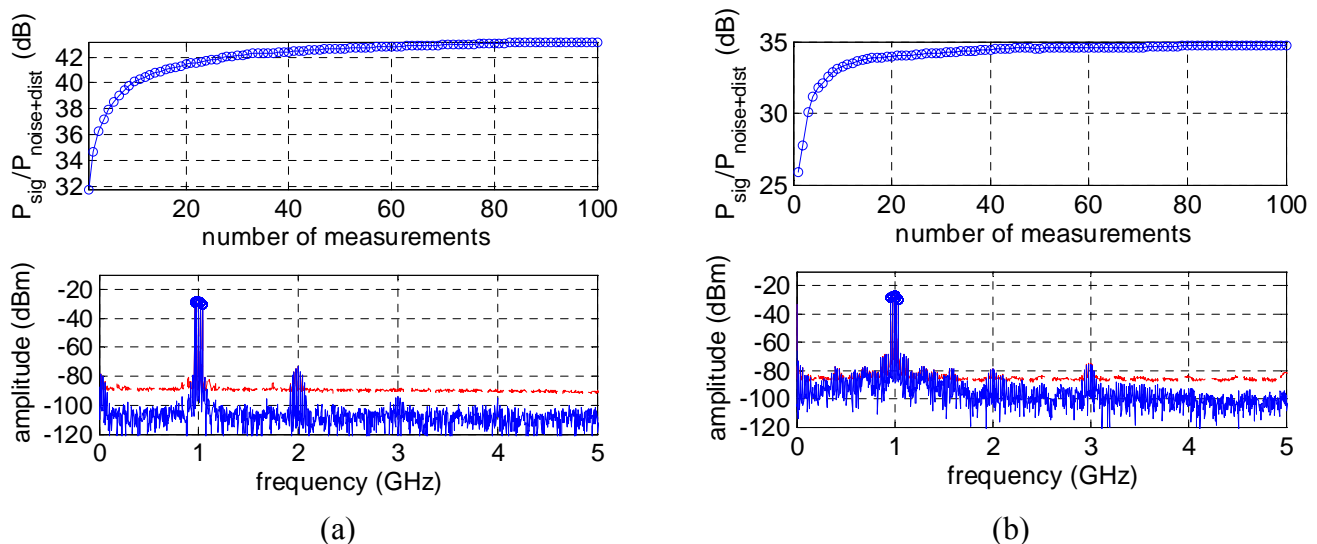
Figure 2: Five-tone multisine with $\Delta f = 20$ MHz. Top graphs show improvement in SINAD with number of time-domain averages. Bottom graphs (blue) show the DFT of the average of 100 measurements. The narrow (red) curve with the higher level is the mean of the 100 magnitude spectra. Averaging the magnitude spectra reduces the variation in the noise, but not the noise floor itself. (a) DSO measurement; (b) SWA measurement.
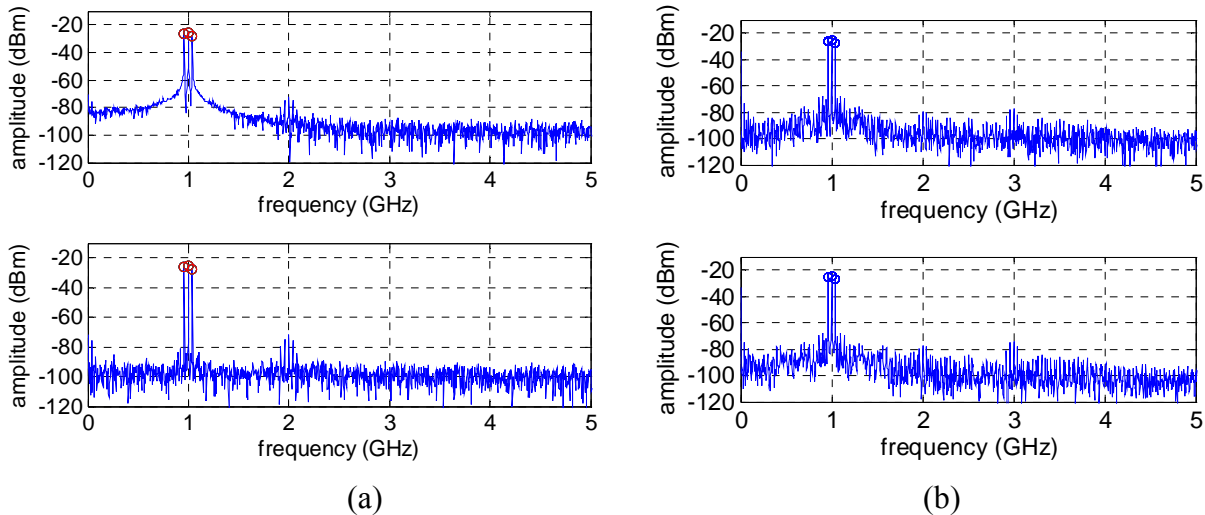
Figure 3: Measurements of the three-tone multisine with frequency spacing of 40 MHz. (a) Oscilloscope measurements with no time-base correction (top) and with time-base and jitter correction (bottom). (b) Sampling Waveform Analyzer measurements without dithering (top) and with dithering (bottom).

interpolation to create an equally spaced time record for the Fourier transform procedure. The spectra of a three-tone multisine measured on the oscilloscope with and without the time-base correction is shown in Fig. 3(a).

C. The Sampling Waveform Analyzer Measurements

The basic mode of operation of the SWA is that of a successive approximation analog-to-digital converter. The SWA uses a custom-designed sampling comparator probe that serves as both the sampler and the decision element. Similar to the DSO, the SWA samples in equivalent time, where one sample is taken at each trigger event and successive triggers are delayed in time. In equivalent-time sampling, the instrument traces out a sampled waveform over several sampling periods. In the SWA, the value of the measured waveform at a given sampling instant is successively approximated to a digitizing resolution of *M* bits through a binary search using *M* successive periods of the waveform.

The SWA has an optional measurement mode that uses a form of dithering to further reduce the overall noise floor. This mode is invoked following the successive approximation process and works by allowing noise at the sampler's input to increase or decrease the system reference value in accordance with the comparator decision at each sampling instant. The amount by which the system reference is increased or decreased is equal to the least significant bit of the successive approximation process. By averaging the dithered reference values over *L* sampling instants, this sampling process achieves the same effective reduction in noise as would be achieved if *L M*-bit data samples were collected. Spectra from both the non-dithered (average of 100 measurements) and dithered modes (average of 10 measurements) are shown in Fig. 3(b).

D. Measurement Results

Table II lists several parameters of interest, including the standard deviation, *s*, of the 100 phase measurements, the SINAD, and the mean values for the second- and third-harmonic distortion. We report the highest value of standard deviation and harmonic distortion among the

frequency components in the multisine. We calculated the standard deviation of the individual measurements as

$$s_x = \sqrt{\frac{1}{N-1}\sum_{i=1}^{N}\left(x_i - \bar{x}\right)^2}. \tag{4}$$

We calculated harmonic distortion by comparing the level of the harmonic to that of the fundamental. Using logarithmic quantities, we define harmonic distortion as

$$HD = V_{harm}(dB) - V_{fund}(dB) \tag{5}$$

The last two columns in Table II give value of intermodulation distortion in sidebands spaced Δf above the highest (IMU) and lowest (IML) frequency components. These sidebands are caused by distortion products from the measurement instrument, the trigger circuit, and the signal generator itself.

The values of standard deviation of the phase measurements in Table II are well within one degree. As expected, the SINAD for the jitter-corrected DSO measurements is better than that of the SWA. The second harmonic distortion is better for the SWA than the scope, while the opposite is true for the third harmonic distortion. Some asymmetry in intermodulation is apparent in almost all of the measurements. Note that the third harmonic distortion is worse for both instruments when the relative phases are constant than when they are Schroeder. The constant-phase multisine has a higher peak-to-average power ratio, which can cause distortion in instrumentation. This is one motivation for using the Schroeder multisine.

Relative phase measurements are shown in Fig. 4. Each graph shows the difference between the measured and specified (target) phases so that we can compare measurements of constant phase and Schroeder phase multisines easily. All 100 measurements are plotted in each graph. Both instruments show differences between specified and measured phases of approximately ±5 degrees for the three-tone, $\Delta f = 40$ MHz multisine and up to ±20 degrees for the 5-tone, $\Delta f = 20$ MHz multisines. The agreement between measurements made on instruments with significantly different architectures gives us an indication that these phase differences are in fact occurring in the VSG and are not measurement error. Measurements such as these let us characterize our VSG at any particular age, firmware version, and point in its calibration cycle, and enables use of the VSG as a calibration source.

Table II: Parameters (defined in the text) for 100 measurements by the SWA and DSO. CC refers to multisines with constant magnitude and constant, zero-degree relative phases, while CS refers to those having Schroeder relative phases. SWA(d) refers to the SWA measurements with dithering (10 total).

Multisine	Instrument	s (deg)	SINAD (dB)	2HD (dB)	3HD (dB)	IML (dB)	IMU (dB)
3 tones, $\Delta f = 40$ MHz, CC	DSO	0.05	43.5	-46.1	-71.7	-55.3	-62.5
	SWA	0.70	35.0	-54.8	-52.5	-50.2	-48.6
	SWA (d)	0.26	34.4	-52.3	-49.5	-48.8	-50.9
5 tones, $\Delta f = 20$ MHz, CC	DSO	0.09	43.2	-45.6	-66.5	-51.0	-52.8
	SWA	0.16	34.8	-50.8	-48.2	-38.6	-50.9
	SWA(d)	0.10	34.8	-50.0	-47.5	-44.2	-41.1
5 tones, $\Delta f = 20$ MHz, CS	DSO	0.08	42.8	-46.6	-76.0	-54.6	-58.4
	SWA	0.20	35.4	-52.6	-60.9	-47.6	-44.7
	SWA(d)	0.16	35.6	-53.6	-61.4	-44.9	-46.2

DSO Measurements

SWA Measurements

(a)

(b)

(c)

(d)

(e)

(f)
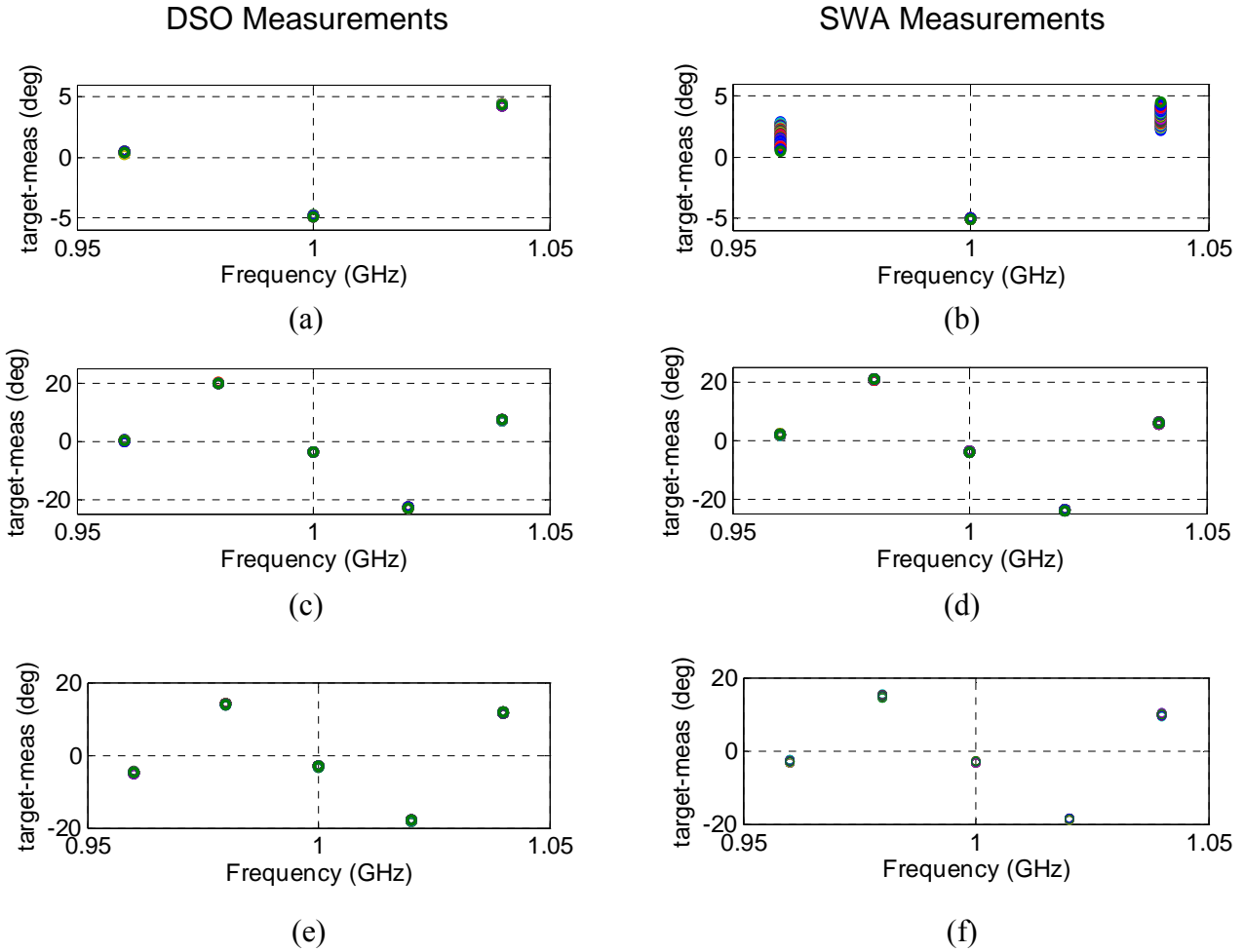
Figure 4: Difference between target and measured phases for all 100 runs. Left graphs show DSO measurements and right show SWA measurements. (a) and (b): a three-tone constant-phase multisine with $\Delta f = 40$ MHz; (c) and (d): a five-tone constant-phase multisine with $\Delta f = 20$ MHz; (e) and (f): a five-tone Schroeder-phase multisine with $\Delta f = 20$ MHz. Note the similar trends in the 5-tone multisine measurements (c) – (f).

IV. NARROWER-BAND MULTISINE MEASUREMENTS

The vector signal analyzer falls into the class of instrument often called Fourier Transform Analyzers or Real-Time Analyzers, since data are collected in the time domain but are transformed into the frequency domain for analysis and display. Unlike the SWA and the DSO which acquire one sample per sampling period, the VSA acquires data by periodically downconverting and sampling long time records. Since the signal is downconverted before being transformed to the frequency domain, fine details can be resolved around the carrier frequency but only within a relatively narrow modulation bandwidth. The measurement bandwidth of the VSA we used is 36 MHz, much narrower than either the SWA or DSO. As a result, harmonic distortion cannot be measured for the multisines we consider here. Because we acquire the frequency-domain coefficients of the measured signal, time-domain averaging was not carried out on the VSA measurements. However, the noise floor of this instrument is inherently lower than the DSO or SWA because of its narrow acquisition bandwidth.
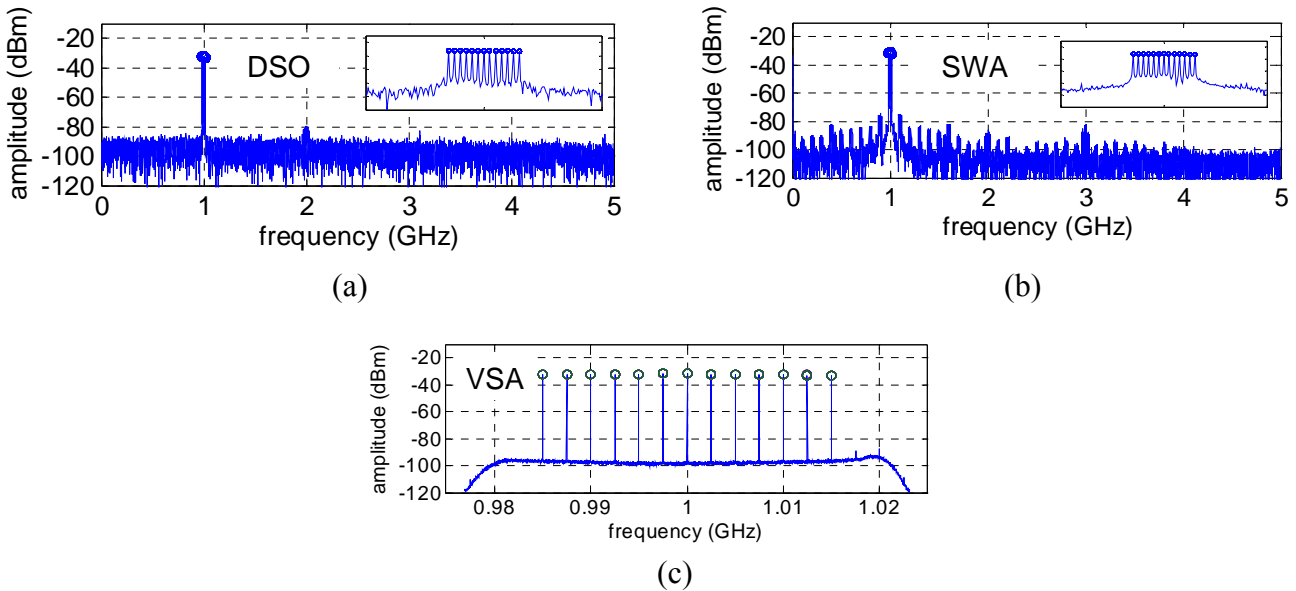
Figure 5: 13-tone, Schroeder-phase multisine measured with (a) the DSO, (b) the SWA, and (c) the VSA. The VSA span was set to 30 MHz, and 6400 points were acquired. Insets show zoomed-in spectra from the DSO and SWA.

One method to accurately measure magnitude and phase of a periodic signal using the VSA is to ensure that the instrument is set up to acquire an even number of envelope periods. We chose the span and resolution bandwidth carefully with this in mind. The magnitude of the DSO-, SWA-, and VSA-measured signals are shown in Fig. 5(a)-(c).

To compare SINAD from measurements made on the VSA, DSO, and SWA, we specified a calculation bandwidth narrower than the full measured spectrum. In each calculation, we included the distortion products IML and IMU spaced Δf above the highest and lowest frequency components. Table III compares measured parameters for the VSA, DSO, and SWA.

Table III shows that the standard deviation for all phase measurements is within 0.5 degree. We see that the SINAD measurements for the DSO and VSA are comparable, but the measured intermodulation distortion products are significantly lower on the VSA than on either the DSO or the SWA. As before, the second harmonic distortion is better for the SWA than the

Table III: Measured parameters (defined in the text) for 100 measurements of multisines by the DSO, SWA, and VSA. CC refers to multisines with constant magnitude and constant, zero-degree relative phases, while CS refers to those having Schroeder relative phases.

Multisine	Instrument	s_{max} (deg)	SINAD (dB)	2HD (dB)	3HD (dB)	IML (dB)	IMU (dB)
3 tones, Δf=2.5 MHz, CC	DSO	0.07	39.4	-46.6	-65.9	-45.2	-46.5
	SWA	0.11	36.9	-51.4	-52.5	-49.6	-43.9
	VSA	0.05	36.6	--	--	-58.2	-57.1
9 tones, Δf=2.5 MHz, CS	DSO	0.12	32.6	-48.0	-69.6	-40.7	-47.4
	SWA	0.38	29.4	-59.6	-53.9	-54.5	-49.8
	VSA	0.12	37.7	--	--	-57.2	-61.0
13 tones, Δf=2.5 MHz, CS	DSO	0.14	35.5	-47.5	-60.9	-43.9	-44.5
	SWA	0.47	29.3	-57.9	-53.3	-48.0	-41.5
	VSA	0.23	35.7	--	--	-55.7	-65.8

scope, while the opposite is true for the third harmonic distortion.

Finally, Fig. 6 shows the difference between measured and target phases for the three-tone and nine-tone multisines made on all three instruments, respectively. The frequency spacing between tones is 2.5 MHz, so these are much more narrowband signals than those described in Section 2. We see that the agreement between measured and target phases is much closer for the narrowest band multisine (the three-tone shown in the left column of Fig. 6). It is more difficult to tell, on these narrow-band measurements, if the difference between specified and measured phases arises from the VSG or the measurement apparatus.
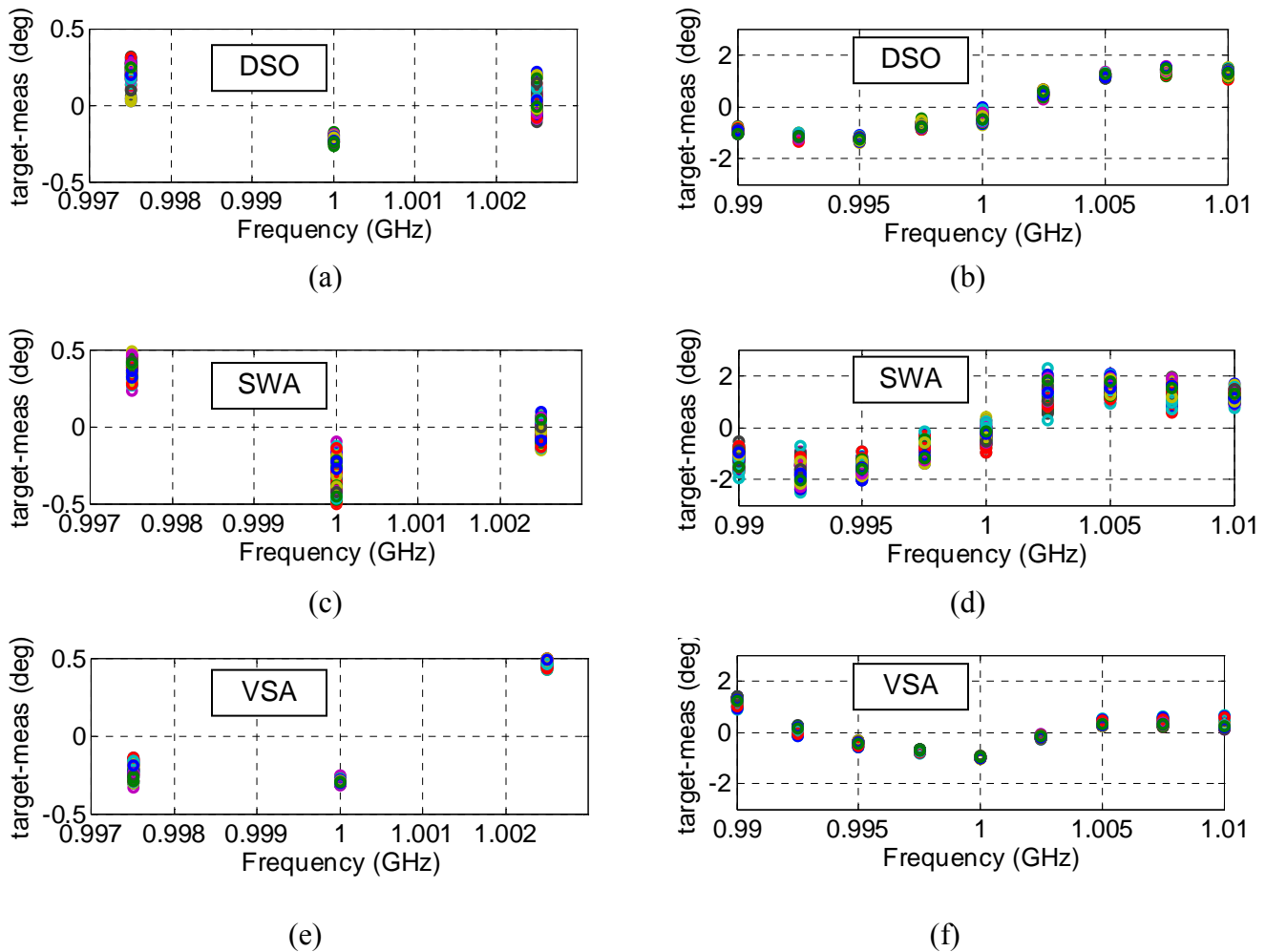
Figure 6: Left-hand plots show the difference between specified and measured relative phases of a three-tone multisine with $\Delta f = 2.5$ MHz. Right-hand plots are for a nine-tone multisine, also with $\Delta f = 2.5$ MHz. (a) and (b): DSO measurements; (c) and (d): SWA measurements; (e) and (f) VSA measurements. Better agreement between measured and specified phases is seen for the narrower-bandwidth signals on the left, although agreement for both multisines is less than ±2 degrees at 1 GHz.

V. Conclusion

This study compared measurements of simple multisines generated by a vector-signal generator. The measurements were made by three instruments capable of measuring both the magnitude and relative phase of distortion products, which is useful in the characterization of nonlinear systems. The digital sampling oscilloscope in our study had a very low signal-to-noise ratio, in part because of a special time-base distortion algorithm utilized during the measurements. Second-harmonic distortion was more prevalent in the sampling oscilloscope than in the sampling waveform analyzer measurements we made. The opposite was true for the third harmonic distortion.

We compared measurements on narrower band multisines using a vector signal analyzer. Measurements made with this instrument had lower intermodulation distortion than those made with either the oscilloscope or the sampling waveform analyzer.

Measurements of relative phase agreed very well between all of the instruments. Differences between the phases we specified on our vector signal generator and those we measured with the various instruments were all similar, indicating that it would be possible to characterize the signal generator for use as a calibration source. The standard deviation in our relative phase measurements was always less than one degree at a 1 GHz carrier frequency, indicating good repeatability from each instrument. This study demonstrated that all three instruments would be suitable for measuring relative phase of both excitation and distortion products of signals arising from nonlinear systems.

References

[1] K.A. Remley, "Multisine excitation for ACPR measurements," *IEEE MTT-S Int. Microwave Symp. Dig.*, June 2003, pp. 2141-2144.

[2] P.D. Hale, C.M. Wang, D.F. Williams, K.A. Remley, J. Wepman, "Compensation of random and systematic timing errors in sampling oscilloscopes," *IEEE Trans. Instrum. and Measurement*, in review.

[3] Time-base correction software available for download at: http://boulder.nist.gov/div815/HSM_Project/HSMP.htm

[4] T. M. Souders et al., "A Wideband Sampling Voltmeter", *IEEE Trans. Instrum.& Meas.*, Vol. 46, No. 4, August 1997, pp. 947-953.

[5] O. B. Laug et al., "A Custom Integrated Circuit Comparator for High-Performance Samplng Applications", *IEEE Trans. Instrum. & Meas.*, Vol. 41, No. 6, December 1992, pp. 850-855.

[6] R. Pintelon and J. Schoukens, "System Identification: A Frequency Domain Approach." New York, NY: IEEE Press, 2001.

[7] K.A. Remley, D. F. Williams, D. Schreurs, G. Loglio, and A. Cidronali, "Phase detrending for measured multisine signals," *61st ARFTG Conf. Dig.*, June 2003, pp. 73-83.